ChemComm

Accepted Manuscript

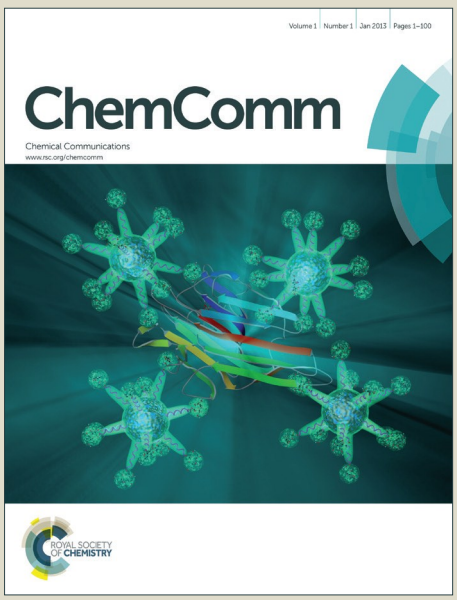

ROYAL SOCIETY OF CHEMISTRY

www.rsc.org/chemcomm

Journal Name

RSCPublishing

COMMUNICATION

Synthesis of nanostructured clean surface molybdenum carbides on graphene sheets as efficient and stable hydrogen evolution reaction catalysts

Cite this: DOI: 10.1039/x0xx00000x

Received xx th xxxxxxxx 20 xx,
Accepted xx th xxxxxxxx 20 xx

DOI: 10.1039/x0xx00000x

www.rsc.org/

Chunyong He[a], Juzhou Tao*[,a]

Small szie molybdenum carbides (2.5 nm for MoC and 5.0 nm for Mo_2C) with clean surface on graphene were prepared for efficient and stable hydrogen evolution reaction catalysts.

Hydrogen is one of the principal candidates for a renewable and eco-friendly energy vector to meet the twin challenges of global climate change and fossil fuel exhaustion.[1] The development of catalysts for use in hydrogen evolution reaction (HER), the elementary reaction for hydrogen production, has therefore attracted much research interest and attention.[2] Although Pt-based catalysts are efficient HER catalysts with high current density at low overpotential,[3] the scarcity and high price of Pt limit their large-scale applications. Among considerable efforts in search for earth-abundant metal based alternatives, some successful examples are transitional metal chalcogenides (MoS_2,[2a] WS_2,[4] $CoSe_2$[5]), phosphides (Ni_2P,[6] Cu_3P,[7] FeP[8]), nitride ($Co_{0.6}Mo_{1.4}N_2$,[9] $NiMoN_x/C$[10]) and metal-free carbon nitride based materials[11].

While molybdenum carbides exhibit HER catalytic activities similar to that of Pt,[12] commercially available micron-sized molybdenum carbides are inadequate as efficient catalysts in practical applications. Further improvements in electro-catalytic activity and stability have been achieved through nanocrystallization,[13] or transition metal (such as Co or Ni) impregnation.[14] The most direct and efficient approach is to decrease grain size of molybdenum carbides. In this communication we report the synthesis of nanostructured molybdenum carbide in small size (2.5 nm for MoC and 5.0 nm for Mo_2C) on graphene support *via* a simple *in situ* approach. The as-synthsized products show a highly dispersed distribution of nanoparticles on the graphene support, which provides a large surface area and high conductivity to the Mo-compounds, thus increasing the HER catalytic activity through enhanced mass and charge transfer.

By optimizing thermal annealing temperature we first prepared molybdenum carbides in different crystalline forms. Fig. 1a displays the X-ray diffraction (XRD) pattern of the MoC on graphene hybrid material (MoC-G), formed at 750 °C. The MoC shows a typical cubic structure (Fm-3m(225)) indicated by the magenta vertical lines (PDF#65-0280). The XRD pattern of Mo_2C with Fe_2N structure (hexagonal, P63/mmc(194)) formed at 900 °C on graphene (Mo_2C-G), as indicated by the red vertical lines (PDF#35-0787), is shown in Fig. 1b.

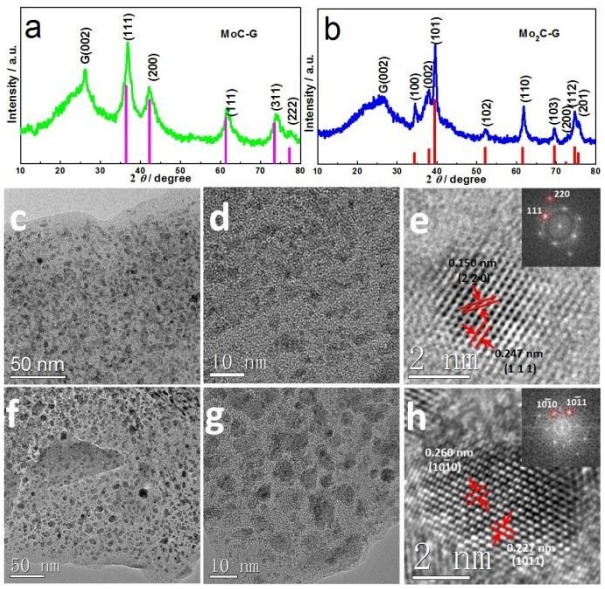

Fig. 1 The XRD patterns of (a) MoC-G and (b) Mo_2C-G, (c, d) TEM images of the MoC-G, (e) HRTEM image of the MoC-G and its corresponding FFT (inset), (f, g) TEM images of the Mo_2C-G, (h) HRTEM image of the Mo_2C-G and its corresponding FFT (inset).

The graphene sheets are interconnected with each other without any agglomeration, resulting in a porous three-dimensional structure with micron and sub-micron size pores conducive to mass transfer (shown in Fig. S1, ESI†). Fig. 1c and 1d show the typical TEM images of the MoC-G composites. The MoC NPs are homogeneously dispersed on the graphene surface, the average diameter of MoC NPs is about 2.5 nm according to particle size distribution (Fig. S2a, ESI†). The high-resolution TEM (HRTEM) image of MoC shows the lattice fringes which measured 0.247 and

0.150 nm, consistent with the (111) and (220) crystal planes of MoC (Fig. 1e), respectively. Inset in Fig. 1e is the corresponding fast Fourier transform (FFT). Fig. 1f and 1g display the typical TEM images of the Mo_2C-G composites, showing a highly dispersed system. Average diameter of Mo_2C NPs is about 5.0 nm according to particle size distribution (Fig. S2b, ESI†). As no other chemical reagents were used in the synthesis process, surface of the MoC and Mo_2C NPs is definitely clean, which is essential to HER activity. From HRTEM image shown in Fig. 1h, the clearly resolved interplanar distances are measured 0.260 nm and 0.227 nm, corresponding to the $(10\bar{1}0)$ and $(10\bar{1}1)$ crystal planes of the Mo_2C, respectively. Inset in Fig. 1h is the corresponding FFT. Table S1 shows the comparison of the crystal planes of MoC and Mo_2C. Fig. S3 (ESI†) shows the energy dispersive spectrometry (EDS) patterns of MoC-G and Mo_2C-G.

Comparison of the Raman spectra of graphene oxide (GO), MoC-G and Mo_2C-G composites in 1000–3000 cm^{-1} range is shown in Fig. S4 (ESI†). The D band at 1350 cm^{-1}, assigned to the Brillouin zone K-point phonons of A1g symmetry, characterizes graphite plane disordering and defect incorporation into the pentagon and heptagon graphitic structures.[15] The band observed at about 1580 cm^{-1} is the G band which corresponds to a splitting of the E_{2g} graphite stretching mode and reflects structural intensity of the sp^2-hybridized carbon atoms.[16] The I_G/I_D ratios of the GO, graphene, MoC-G and Mo_2C-G composites are 0.78, 1.54, 1.25 and 1.28, respectively. The increased I_G/I_D ratio relative to GO indicates the reduction of GO to graphene formation.[17]

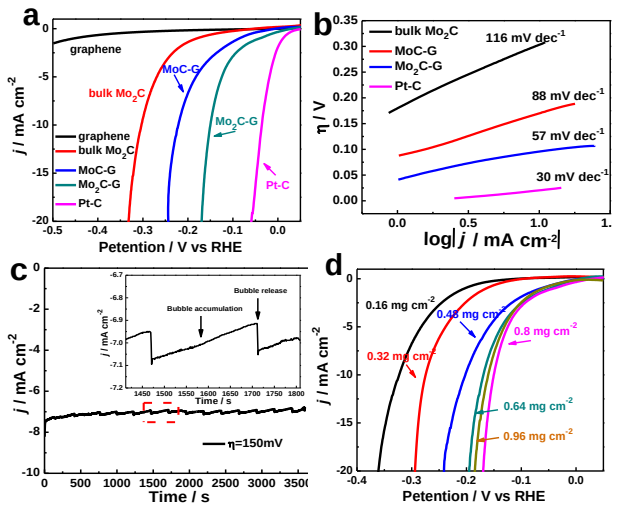

Fig. 2 (a) Polarization curves of bulk Mo_2C, MoC-G, Mo_2C-G , Pt/C and graphene, (b) Tafel plots obtained from the polarization curves of various catalysts, (c) Time dependence of current density under static overpotential of 160 mV, Inset: enlargement of the area marked by the dash box, (d) The polarization curves of the Mo_2C-G catalyst under different loadings.

HER behavior of the bulk Mo_2C, MoC-G, Mo_2C-G , Pt/C and graphene were investigated on a glassy carbon electrode in 0.5 mol L^{-1} H_2SO_4 solution. As shown in Fig. 2a, the Pt/C catalyst exhibited the best HER activity. The graphene barely shows electrocatalytic activity towards the HER, but dramatically improves after introduction of molybdenum carbides, as indicated by the exceptional HER activity of Mo_2C-G with a small overpotential (η_{10}) of 150 mV at 10 mA cm^{-2} and a small overpotential (η_{20}) of 170 mV at 20 mA cm^{-2}. The η_{10} of bulk Mo_2C is 304 mV, also much higher than that of Mo_2C-G. To our best knowledge, Mo_2C with Fe_2N structure is about the only form of molybdenum carbide studied as catalyst for HER,[12b] we hereby demonstrate both a new record of the onset overpotential with Mo_2C-G and the HER activity of a new phase of molybdenum carbide (cubic, Fm-3m(225)) nanoparticles on graphene (MoC-G). Fig. 2a also shows that the onset overpotential of the MoC-G is close to that of the Mo_2C-G. The overpotential (η_{10}) of MoC-G at 10 mA cm^{-2} of cathodic current density is 221 mV. Comparison of the HER perfomance of the various catalysts are summarized in table S2.

To discern the predominant HER mechanism of the various catalysts, Tafel plots were fitted to Tafel equation ($\eta = a+b*\log|j|$), where j is the current density and b is the Tafel slope. In acidic solution, hydrogen evolves through a multi-step process on the surface of an electrode, as shown in Scheme S1. The first step of HER is the Volmer or discharge reaction with electron from external circuit transferring to the catalyst surface and coupling to a proton to yield an absorbed hydrogen atom: $H_3O^+ + e^- \rightarrow H_{abs} + H_2O$. The following step is the formation of H_2, which may occur via two different reaction pathways. One is the Tafel or combination reaction, in which two absorbed hydrogen atoms combine on the catalyst surface: $H_{abs} + H_{abs} \rightarrow H_2$. The other is the Heyrovsky or ion + atom reaction, in which a second electron from external circuit transfers to the catalyst surface where an absorbed hydrogen atom couples to a proton to yield H_2: $H_3O^+ + e^- + H_{abs} \rightarrow H_2 + H_2O$. Fig. 2b displays the Tafel plots for HER on bulk Mo_2C, MoC-G, Mo_2C-G and Pt/C electrodes. The Tafel slope of Pt/C is 30 mV dec^{-1} and found identical to previously reported values[14,17], and the HER on a Pt surface is understood as proceeding through the Volmer–Tafel reaction mechanism, the discharge reaction is fast and H_2 is evolved by a rate-determining combination reaction or Tafel step[18]. The Tafel slope of bulk Mo_2C is 116 mV dec^{-1} and consistent with the previous reported values[17,19], which suggests that the discharge reaction is slow and Volmer step is the rate-determining step. The observed Tafel slope of 57 mV dec^{-1} for Mo_2C-G is comparable to the previously reported values of 58 mV dec^{-1} for Mo_2C/CNT-GR[17], 64 mV dec^{-1} for Mo_2C-CNT[13], 58 mV dec^{-1} for Mo_2C-R[14] and 62.7 mV dec^{-1} for MoSoy/RGO[12a]. This value is much smaller than that of bulk Mo_2C, suggesting correspondingly faster proton discharge kinetics. The Tafel slope of MoC-G is 88 mV dec^{-1}, which is smaller than previously reported γ-MoC (hexagonal strucure, P-6m2, 121.6 mV dec^{-1})[19]. With the Tafel slope values of 57 mV dec^{-1} and 88 mV dec^{-1}, one possible pathway for HER on MoC-G and Mo_2C-G catalysts is through a Volmer–Heyrovsky reaction mechanism, the rate determining step could be discharge reaction or the electrochemical desorption of H_{ads} and H_3O^+ to form hydrogen.

An ideal HER catalyst requires low onset overpoential, small Tafel slope and large exchange current densities (j_0), which represent high and intrinsic catalytic activities for HER. As shown in table S2, the j_0 of the MoC-G and Mo_2C-G are 2.55×10^{-2} mA cm^{-2} and 2.58×10^{-2} mA cm^{-2}, which are about one order of magnitude higher than 3.79×10^{-3} mA cm^{-2} for bulk Mo_2C, representing their significantly improved HER catalytic activity. The fast electron transport offered by graphene is likely the origin of the higher exchange current densities in MoC-G and Mo_2C-G catalysts. The turnover frequency (TOF) of the MoC-G and Mo_2C-G are0.036 s^{-1} and 0.041 s^{-1} (at 0 mV vs RHE), respectively. These values are not much lower than that of Pt (111) surface (TOF = 0.9 s^{-1}, at 0 mV vs RHE)[20] and highr than MoS_2 edge (0.02 s^{-1}, at 0 mV vs RHE)[20] Ni_2P nanoparticles (0.015 s^{-1}, at -100 mV vs RHE)[21].

Fig. 2c shows the *i-t* chronoamperometric response for the Mo_2C-G at the overpotential of 160 mV. The as-measured *i-t* curve is in typical serrate shape, which results from the alternating processes of bubble accumulation and bubble release. The current density differs by less than 0.2 mA cm^{-2} before and after release, indicating that the bubbles can be easily released on the surface of the Mo_2C-G. This efficient bubble release is likely originated from the porous structure of the Mo_2C-G. The HER activity of the Mo_2C-G was further evaluated by depositing catalyst on the glassy carbon electrode at different loadings. Fig. 2d shows the optimal loading is 0.8 mg cm^{-2}.

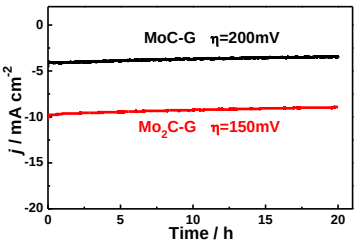

Fig. 3 Stability test of the MoC-G and Mo_2C-G catalysts.

High durability in acid media is also a challenge to the Mo-based compounds in their practical application. The long-term stability of the MoC-G and Mo_2C-G catalysts were examined by extended electrolysis at fixed overpotentials and shown in Fig. 3. After a long period of 20 h, the current density on the MoC-G and Mo_2C-G electrodes only show negligible degradation, which could be due to the consumption of proton in the system and the hindrance of the reaction by hydrogen bubbles remaining on the electrodes. The cyclic voltammograms of MoC-G and Mo_2C-G electrodes obtained before and after 2,000 cycles are shown in Fig. S5. No obvious degradation on both MoC-G and Mo_2C-G electrodes. The high durability of the MoC-G and Mo_2C-G mianly originates from: 1) the coupling effect between molybdenum carbides and graphene; 2) the tight anchoring result fom the *in situ* synthesis method.

Conclusions

We report the synthesis of nanostructured molybdenum carbides with clean surface on graphene *via* a simple *in situ* method. The sizes of the MoC and Mo_2C are 2.5 nm and 5.0 nm, respectively, which are much smaller than those of molybdenum carbides previously reported. The MoC-G and Mo_2C-G show extraordinary high acitivity for HER with negligible onset overpotentials (15 mV for the MoC-G and nearly zero onset overpotential for the Mo_2C-G), also the smallest onset overpotentials in existing literature. In addition, both the MoC-G and Mo_2C-G exhibit superior durability. The outstanding performance of MoC-G and Mo_2C-G for HER is attributed to the large number of active sites due to the small sizes, fast available electron transfer capabilities offered by graphene, clean surfaces of the MoC and Mo_2C nanoparticles and the porous microstructure. The MoC-G and Mo_2C-G are promising non-precious metal catalysts for HER with their good activity, high stability, and low price.

This work was supported by the 100 Talents Project of Chinese Academy of Sciences, China (H9291440S3).

Notes and references

[a] Dongguan Neutron Science Center, Institute of High Energy Physics, Chinese Academy of Sciences, Dongguan 523808, China. Fax: +86 769 89156463; Tel: +86 769 89156463; E-mail: taoj@ihep.ac.cn

† Electronic Supplementary Information (ESI) available: Experimental section and Additional experimental data. See DOI: 10.1039/b000000x/

1 (a) M. S. Dresselhaus and I. L. Thomas, *Nature*, 2001, **414**, 332; (b) A. R. J. Kucernak and V. N. Naranammalpuram Sundaram, *J. Mater. Chem. A*, 2014, **2**, 17435.
2 C. G. Morales-Guio, L.-A. Stern and X. Hu, *Chem. Soc. Rev.*, 2014, **43**, 6555.
3 R. Subbaraman, D. Tripkovic, D. Strmcnik, K. C. Chang, M. Uchimura, A. P. Paulikas, V. Stamenkovic and N. M. Markovic, *Science*, 2011, **334**, 1256.
4 D. Voiry, H. Yamaguchi, J. Li, R. Silva, D. C. B. Alves, T. Fujita, M. Chen, T. Asefa, V. B. Shenoy, G. Eda and M. Chhowalla, *Nat. Mater.*, 2013, **12**, 850.
5 D. Kong, H. Wang, Z. Lu and Y. Cui, *J. Am. Chem. Soc.*, 2014, **136**, 4897.
6 E. J. Popczun, J. R. McKone, C. G. Read, A. J. Biacchi, A. M. Wiltrout, N. S. Lewis and R. E. Schaak, *J. Am. Chem. Soc.*, 2013, **135**, 9267.
7 J. Tian, Q. Liu, N. Cheng, A. M. Asiri and X. Sun, *Angew. Chem. Int. Ed.*, 2014, n/a.
8 R. Liu, S. Gu, H. Du, A. M. Asiri and C. Li, *J. Mater. Chem. A*, 2014.
9 B. Cao, G. M. Veith, J. C. Neuefeind, R. R. Adzic and P. G. Khalifah, *J. Am. Chem. Soc.*, 2013, **135**, 19186.
10 W.-F. Chen, K. Sasaki, C. Ma, A. I. Frenkel, N. Marinkovic, J. T. Muckerman, Y. Zhu and R. R. Adzic, *Angew. Chem. Int. Ed.*, 2012, **51**, 6131.
11 Y. Zheng, Y. Jiao, Y. Zhu, L. H. Li, Y. Han, Y. Chen, A. Du, M. Jaroniec and S. Z. Qiao, *Nat. Commun.*, 2014, **5**.
12 (a) W.-F. Chen, S. Iyer, S. Iyer, K. Sasaki, C.-H. Wang, Y. Zhu, J. T. Muckerman and E. Fujita, *Energy Environ. Sci.*, 2013, **6**, 1818; (b) W.-F. Chen, J. T. Muckerman and E. Fujita, *Chem. Commun.*, 2013, **49**, 8896.
13 (a) W. F. Chen, C. H. Wang, K. Sasaki, N. Marinkovic, W. Xu, J. T. Muckerman, Y. Zhu and R. R. Adzic, *Energy Environ. Sci.*, 2013, **6**, 943; (b) L. F. Pan, Y. H. Li, S. Yang, P. F. Liu, M. Q. Yu and H. G. Yang, *Chem. Commun.*, 2014, **50**, 13135.
14 P. Xiao, Y. Yan, X. Ge, Z. Liu, J.-Y. Wang and X. Wang, *Appl. Catal., B : Environ.*, 2014, **154-155**, 232.
15 F. Banhart, J. Kotakoski and A. V. Krasheninnikov, *ACS Nano*, 2010, **5**, 26.
16 L. Can çado, A. Reina, J. Kong and M. Dresselhaus, *Phys. Rev. B*, 2008, **77**.
17 D. H. Youn, S. Han, J. Y. Kim, J. Y. Kim, H. Park, S. H. Choi and J. S. Lee, *ACS Nano*, 2014, **8**, 5164.
18 Y. Li, H. Wang, L. Xie, Y. Liang, G. Hong and H. Dai, *J. Am. Chem. Soc.*, 2011, **133**, 7296.
19 C. Wan, Y. N. Regmi and B. M. Leonard, *Angew. Chem. Int. Ed.*, 2014, **53**, 6407.
20 T. F. Jaramillo, K. P. Jorgensen, J. Bonde, J. H. Nielsen, S. Horch and I. Chorkendorff, *Science*, 2007, **317**, 100.
21 E. J. Popczun, J. R. McKone, C. G. Read, A. J. Biacchi, A. M. Wiltrout, N. S. Lewis and R. E. Schaak, *J. Am. Chem. Soc.*, 2013, **135**, 9267.

The table of contents entry

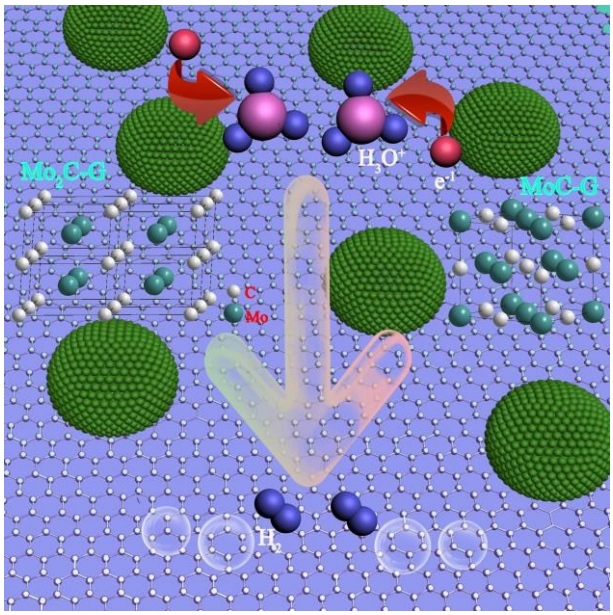

The MoC-G and Mo_2C-G are promising non-precious metal catalysts for HER with their good activity, high stability, and low price.